RadioGraphics

Restaging Locally Advanced Rectal Cancer with MR Imaging after Chemoradiation Therapy[1]

TEACHING POINTS
See last page

Brunella Barbaro, MD • Renata Vitale, MD • Lucia Leccisotti, MD
Fabio M. Vecchio, MD • Luisa Santoro, MD • Vincenzo Valentini, MD
Claudio Coco, MD • Fabio Pacelli, MD • Antonio Crucitti, MD
Roberto Persiani, MD • Lorenzo Bonomo, MD

In recent years, preoperative therapy has become standard procedure for locally advanced rectal cancer. Tumor shrinkage due to preoperative chemotherapy–radiation therapy (CRT) is now a reality, and pathologically complete responses are not uncommon. Some researchers are now addressing organ preservation, thus increasing the demand for both functional and morphologic radiologic evaluation of response to CRT to distinguish responding from nonresponding tumors. On magnetic resonance (MR) images, post-CRT tumor morphologic features and volume changes have a high positive predictive value but a low negative predictive value for assessing response. Preliminary results indicate that diffusion-weighted MR imaging, especially at high *b* values, would be effective for prediction of treatment outcome and for early detection of tumor response. Some authors have reported that the use of apparent diffusion coefficient values in combination with other MR imaging criteria significantly improves discrimination between malignant and benign lymph nodes. Sequential determination of fluorodeoxyglucose uptake at positron emission tomography/computed tomography has proved useful in differentiating responding from nonresponding tumors during and at the end of CRT. However, radionuclide techniques have limitations, such as low spatial resolution and high cost. Large studies will be needed to verify the most effective morphologic and functional imaging modalities for post-CRT restaging of rectal cancer. Supplemental material available at *http://radiographics.rsna.org/lookup/suppl/doi:10.1148/rg.303095085/-/DC1*.

Abbreviations: ADC = apparent diffusion coefficient, CRM = circumferential resection margin, CRT = chemotherapy–radiation therapy, FDG = fluorodeoxyglucose, FOV = field of view, H-E = hematoxylin-eosin, ROI = region of interest, SUV = standardized uptake value, TRG = tumor regression grade

RadioGraphics 2010; 30:699–721 • **Published online** 10.1148/rg.303095085 • **Content Codes:** GI MR OI RO

[1]From the Departments of Bioimaging and Radiological Sciences (B.B., R.V., L.L.,V.V., L.B.), Pathology (F.M.V., L.S.), and Surgery (C.C., F.P., A.C., R.P.), Catholic University, School of Medicine, Largo A. Gemelli 1, 00168 Rome, Italy. Presented as an education exhibit at the 2008 RSNA Annual Meeting. Received April 7, 2009; revision requested July 14; final revision received November 12; accepted November 18. All authors have no financial relationships to disclose. **Address correspondence to** B.B. (e-mail: *bbarbaro@rm.unicatt.it*).

See the commentary by Tudorica et al following this article.

Introduction

Colorectal cancer is the third most common cancer worldwide (1). In the United States, it was estimated that about 145,000 new cases and 56,000 related deaths occurred in 2005 (2). Around 30% of all colorectal cancers are diagnosed in the rectum, and rectal cancer has a worse prognosis for both metastases and local recurrence than does colon cancer (3).

The extraperitoneal rectum (mid- and lower rectum) is surrounded by fatty tissue known as the mesorectum. The mesorectal fascia, or fascia propria of the rectum, is a layer of fibroareolar tissue that surrounds the mesorectum; it represents the circumferential resection margin (CRM) and acts as a natural barrier to tumor spread. Treating both mid- and lower rectal tumors is challenging, and achieving surgical removal with a clear CRM is the goal for the entire multidisciplinary team (4).

Tumor staging is crucial for prognosis and treatment planning. Rectal cancer staging is based on the TNM and UICC (International Union Against Cancer) staging systems (Tables 1, 2). There are two independent predictors: the local status of the tumor (T stage) and the presence or absence of metastatic nodes (N stage). Early-stage (T1 and T2) tumors are neoplasms limited to the rectal wall. In differentiating T2 from T3 tumors, the crucial criterion is infiltration of perirectal fat. Stage T3 tumors pose a greater risk for local recurrence, and the present T staging system does not discriminate between tumors with a wide CRM and those with a close or involved CRM. It has been repeatedly shown that the distance from the tumor to the circumferential mesorectal resection plane is a more powerful predictor for local recurrence than is the T stage. Quirke et al (5) demonstrated that microscopically positive resection margins resulted in a local recurrence rate of 83%. Stage T4 tumors are defined as neoplasms extending beyond the rectal wall, with infiltration of surrounding organs or structures or perforation of the visceral peritoneum. Although en bloc resection of the neoplasm and adjacent organs is performed in these patients, the local recurrence rate remains high (6). Nodal disease is an independent adverse prognostic factor for patient survival and local disease recurrence.

Table 1
TNM Classification of Colorectal Cancer

Type	Description
T1	Tumor invades submucosa
T2	Tumor involves muscularis propria
T3	Tumor extends beyond muscularis propria
T4	Tumor extends to peritoneal surface or invades adjacent organ
N0	No involved nodes
N1	Up to three perirectal or colonic nodes
N2	Four or more perirectal or colonic nodes

As a result, preoperative therapy has gained acceptance in recent years as the standard therapy for rectal cancer (7,8). With the worldwide adoption of preoperative radiation therapy, preoperative staging is important for distinguishing between patients who need only surgery and those who will be at high risk for local disease recurrence without preoperative therapy (9).

Magnetic resonance (MR) imaging is the most promising imaging modality for assessing the most important risk factors for local recurrence: T stage and CRM (10–12). Identifying nodal disease is still a diagnostic problem for radiologists.

Locoregional tumor control in rectal cancer surgery has changed dramatically during the past 10–15 years, starting with discussions of the value of more exact surgical procedures that follow the embryonic planes. This surgical technique is called total mesorectal excision (13). With use of this technique, locally radical surgery can easily be performed without compromising sphincter function in patients with a tumor in the upper and middle third of the rectum. Sphincter preservation is questionable for tumors in the lower third of the rectum. Because the mesorectum decreases in size near the top of the anal canal, tumors in this area can easily invade surrounding structures.

Chemotherapy–radiation therapy (CRT) with delayed surgery will increase the likelihood of preserving sphincter function due to a downsizing and downstaging effect of induction therapy on the tumor, leading to improved resectability and local control (14). Tumor shrinkage due to preoperative CRT is now a reality, and pathologically complete responses are not uncommon (15,16).

Table 2
UICC Staging of Rectal Carcinoma

Stage	Description		
	Tumor	Node	Metastasis
0	Tis	N0	M0
I	T1, T2	N0	M0
IIA	T3	N0	M0
IIB	T4	N0	M0
IIIA	T1, T2	N1	M0
IIIB	T3, T4	N1	M0
IIIC	Every T	N2	M0
IV	Every T	Every N	M1

Note.—UICC = Union Internationale Contre le Cancer (International Union Against Cancer).

Teaching Point

Some researchers are now addressing organ preservation by using preoperative CRT followed by local excision in patients in whom *(a)* CRT has led to downstaging of tumors to lesions confined to the rectal wall, and *(b)* there are no longer any involved lymph nodes (17,18). Furthermore, transanal endoscopic microsurgery has been adopted in patients who otherwise would have undergone abdominoperineal resection (19). Thus, the major challenge for radiologists is to provide a tool to identify those tumors that, after CRT, are most suitable for local excision—namely, tumors confined to the rectal wall (20).

It is also uncertain whether local excision can be avoided if the tumor has responded completely to radiation therapy. Careful follow-up with a "wait and see" approach has produced impressive results, similar to those of radiation therapy for anal carcinoma (21).

Therefore, prediction and early monitoring of treatment effect is a prerequisite for individualized therapy, to steer patients with nonresponding tumors toward more aggressive neoadjuvant treatment.

Presurgical assessment of response may have relevant consequences for treatment planning and prognosis. Thus, increasing demands are being placed on imaging modalities, involving both functional and morphologic evaluation of therapy response, for differentiation of responding from nonresponding tumors after CRT. A new question is now being posed by the multidisciplinary team: How and when should rectal cancer be restaged after CRT?

In this article, we describe the role of imaging in the restaging of rectal cancer after preoperative CRT. In particular, we discuss and illustrate the posttreatment appearances of preoperative rectal cancer at MR imaging, using histopathologic analysis as the standard of reference. We also discuss the capacity of diffusion-weighted MR imaging to help monitor treatment response and whether diffusion-weighted MR imaging can replace positron emission tomography (PET) in this context.

Technical Considerations

We acquired MR imaging data on a 1.5-T unit (Horizon Advantage; GE Medical Systems, Milwaukee, Wis). We used a sagittal localizing image for the selection of transverse and coronal images, all of which were acquired with a fast spin-echo T2-weighted sequence (repetition time msec/echo time msec, 2500–5000/100; matrix, 256 × 256; echo train length, 16; four signals averaged). Coronal and sagittal images were obtained with a 24-cm field of view (FOV), 4-mm-thick sections, and an intersection gap of 1 mm. Axial images were obtained with a 40-cm FOV, 4-mm-thick sections, and an intersection gap of 0.5 mm, so as to match these images with diffusion-weighted MR images.

In addition, oblique high-resolution images were acquired in a plane orthogonal to the tumor with a fast spin-echo T2-weighted sequence (2500/5000; inversion time, 100 msec; matrix, 256 × 256; echo train length, 16). These images were obtained with an 18-cm FOV, 3-mm-thick sections, no intersection gap, and four signals averaged. Axial and coronal T2-weighted sequences with a large FOV were used to image the entire pelvis. T1-weighted sequences were omitted from the standard MR imaging protocol. The total imaging time was 20–25 minutes.

Luminal distention can be achieved with air insufflation or rectal administration of positive or negative contrast material (22). Some authors have recommended no luminal distention (23,24); in our opinion, however, rectal distention permits clear visualization of neoplastic lesions (25,26). Air insufflation may generate susceptibility artifacts; therefore, we use rectal administration of a small amount of sonography

transmission gel to distend the rectal lumen and limit the amount of luminal air. The merits of sonography transmission gel include its inertness in the magnetic field; its high contrast at T2-weighted imaging; its semisolid state, which effectively distends the lumen; and its low cost (25).

Criteria for the Assessment of Response

Methods for assessing response following oncologic therapies continue to evolve. Although tumor size remains the standard of reference, surrogates have been adopted to evaluate tumor necrosis for early response evaluation and residual tumor restaging at the end of treatment. In the following sections, morphologic and diffusion-weighted MR imaging changes are compared with metabolic activity at fluorodeoxyglucose (FDG) PET (both modalities are performed during and at the end of long-course CRT), with histopathologic results as the standard of reference.

Decrease in Tumor Size and Reduction of Tumor Volume

Response evaluation with diagnostic imaging has evolved over the past 25 years (27). In 1979, the World Health Organization introduced, as a criterion for treatment response, a decrease of at least 50% in the cross-product of the maximum diameter and maximum perpendicular dimension of the tumor (28). In 2000, investigators published the Response Evaluation Criteria in Solid Tumors, which included a decrease of at least 30% in maximum diameter (29). Although these two criteria are the most straightforward, inconsistencies arise in measuring geometrically irregular tumors. Because the measurement of multilobed tumors cannot be reproduced, interobserver variability may be unacceptably high. Volumetric analysis provides reliable and more reproducible data than do conventional measurements, which may be affected by the anatomy of the viscera and the intrinsic irregularity of tumor shape (26). Tumor volumes are calculated on oblique high-resolution T2-weighted MR images by manually tracing the lesion on the pertinent images. On each section, areas of the lesion are defined as regions of altered signal intensity and contour relative to the normal adjacent rectal wall. The lesion volumes are displayed automatically in three dimensions and are determined by summing all of the cross-sectional volumes (calculated by multiplying cross-sectional area by section thickness) for the entire lesion (see Fig E1 [online]).

According to standard oncologic criteria, a volume reduction of 65% represents a partial response (29). In our experience with locally advanced rectal cancer, a tumor volume reduction of 70% or more after CRT had a high positive predictive value but a low negative predictive value for distinguishing between responding and nonresponding tumors (26).

Histopathologic Features of Resected Treated Specimens

The use of preoperative CRT modifies the macro- and microscopic aspects of the tumor appearance of rectal cancer. During rectal cancer regression, carcinoma cells are replaced by fibrous or fibroinflammatory tissue. The features of treated tumors include *(a)* marked fibrosis with or without the apparent replacement of neoplastic cells by inflammatory cells, and *(b)* lack of active tumor necrosis but increased mucin production and stromal mucin pools (30). The College of American Pathologists Consensus Statement (31) recommends that mucin production be regarded as a type of treatment response, and that pure acellular mucin be regarded as indicating no residual tumor. Mucinous differentiation due to CRT does not appear to be a poor prognostic factor (32), unlike mucinous untreated rectal carcinoma (33,34). The pathologic stage of the residual tumor (ypT) is determined from the deepest residual viable tumor (according to the TNM system) based on the location of residual cells in the rectal wall or mesorectum. Lymph nodes are categorized as either positive or negative.

Whether a pathologic response to treatment is prognostically significant is determined on the basis of the amount of residual viable tumor versus the amount of fibrous or fibroinflammatory tissue within the gross tumor. There are a number of suggested methods for assessing tumor regression grade (TRG), which represents a modification of the scoring system developed by Mandard et al (35) for esophageal carcinoma: TRG 1 (complete regression) is characterized by the absence of residual cancer and the presence of fibrosis extending through the different layers of the esophageal wall; TRG 2, by the presence of rare residual cancer cells scattered throughout the fibrosis; TRG 3, by an increase in the num-

Table 3
Morphologic MR Imaging Criteria for Tumor Restaging

Criterion	Description
Active tumor	Intermediate signal intensity (higher than that of muscle)
Tumor response	Decreased signal intensity relative to pre-CRT findings, increased signal intensity relative to pre-CRT findings (higher than that of fat)
T2 or less (T0–T2)	Complete disappearance of tumor (normal rectal wall), hypointense thickened rectal wall with or without hypointense spiculations that extend to the perirectal fat
T3	Broad-based pushing or nodular configuration of lateral tumor margin with signal intensity greater than that of muscle extending into perirectal fat
T4	Broad-based pushing or nodular configuration of lateral tumor margin with signal intensity greater than that of muscle extending into an adjacent structure or viscus

ber of residual cancer cells, but with fibrosis still predominant; TRG 4, by residual cancer outgrowing fibrosis; and TRG 5, by the absence of regressive changes. Tumor regression after CRT is assessed by examining the residual neoplastic cells and scoring the degree of both cytologic and stromal changes, including fibrosis with or without inflammatory infiltrate. A finding of few or no tumor cells is associated with a much better outcome after therapy (36). It may be possible to simplify this protocol to distinguish tumors with an excellent response (ie, no residual tumor cells or tumor cells that are difficult to find microscopically [Mandard TRG 1 and 2]) from those with a poor response (ie, easily identifiable tumor cells or no response at all [Mandard TRG 3–5]).

Anatomic MR Imaging Features

On T2-weighted images, the untreated tumor has an intermediate signal intensity between that of the fat tissue (high signal intensity) and that of the muscular layer (low signal intensity), and it invades mesorectal fat with a nodular growth pattern. It is difficult to stage borderline tumors as stage T2 or initial stage T3 with MR imaging; therefore, the goal of staging rectal tumors with MR imaging is to identify patients with bulky stage T3 lesions, a subset with potential CRM involvement, and "T4" patients who might benefit from neoadjuvant treatment. A recent European multicenter rectal MR imaging study (MERCURY trial) (12) concluded that patients with more than 5 mm of extramural spread (stage T3c or T3d) should be identified because they have a markedly worse prognosis than do patients who have stage T3 tumors with 5 mm or less of spread (stage T3a or T3b); therefore, we consider bulky stage T3 tumors to be those with more than 5 mm of spread beyond the outer muscular layer. A distance of less than 2 mm from the adjacent mesorectal fascia is considered to indicate potential CRM involvement (26). In stage T4 tumors, the signal intensity of the tumor is seen infiltrating surrounding organs or structures. On T2-weighted images, the signal intensity of untreated mucinous rectal tumors is higher than that of nonmucinous tumors, which in turn is higher than that of surrounding fat, presumably as a result of the presence of extracellular mucin (37).

At posttreatment MR imaging, the signal intensity characteristics of the major tumor component as well as of the invading, most peripheral portion of the tumor are subjectively assessed relative to the gluteal muscle. Most tumors develop fibrosis, leading to a reduction in T2 signal and a decrease in tumor size. A decrease in signal intensity relative to the pretreatment findings represents a fibrotic response (ie, replacement of neoplasm by fibrosis) (26). Table 3 shows the morphologic MR imaging criteria for tumor restaging. Complete disappearance of the tumor and a thickened hypointense rectal wall are classified as yT0–T2 lesions. The fibrous tissue present after treatment causes thickening of the rectal wall in most cases; thus, MR imaging cannot readily help differentiate stage T0 or T1 tumors from stage T2 tumors because the visualization of individual rectal wall layers is not possible (see Fig E2 [online]) (26). The interface between the

tumor and neighboring organs is classified as either *(a)* spiculations, defined as tiny hypointense strands that stretch from the tumor to the perirectal fat or neighboring organ or structures and represent a response; or *(b)* nodular growth, in which the tumor invades perirectal fat or adjacent structures in an intermediately hyperintense nodular pattern as residual tumor (38). The interpretation of fibrosis with or without residual tumor on MR images remains difficult (see Fig E3 [online]) (20,26,39).

Some treated tumors develop a "colloid" response with mucin production that results in very high signal intensity on T2-weighted images, a finding that is potentially confusing. When MR imaging is used for posttreatment restaging, an increase in tumor signal intensity relative to pretreatment MR imaging findings is generally considered indicative of a mucinous response (40,41). This finding is not to be confused with the markedly hyperintense areas seen on pretreatment MR images, which represent pretreatment mucinous tumors. Irradiated tumors may show a mucin component of up to 80%–90%; thus, it is possible to recognize posttreatment mucinous differentiation on MR images as mucin lakes with markedly increased signal intensity (Fig 1) (42). However, MR imaging for restaging is unable to help differentiate mucinous response or fibroinflammatory tissue from residual tumor, all of which show persistent intermediate signal intensity (see Fig E4 [online]) (43).

MR imaging is considered to be the most accurate tool for the primary staging of tumor extent (10–12). However, it is not accurate in helping distinguish between ypT0, ypT1, and ypT2 tumors at rectal cancer restaging performed after CRT, especially when there is fibrotic thickening of the rectal wall. The main source of error is overstaging (44,45). A reasonable level of accuracy has been achieved with phased-array MR imaging when the end point is differentiating ypT0–T2 tumors from ypT3 tumors, especially when morphologic and volumetric criteria are combined (20,26). It is difficult to restage T3 tumors that may have regressed from the mesorectal fascia, and posttreatment mucinous differentiation and inflammation may cause restaging errors in patients with overstaged disease (see Fig E4 [online]) (26).

Teaching Point

It is impossible to accurately distinguish malignant from benign lymph nodes by relying on size measurements alone. Any proposed cut-off value has been the result of striking a compromise between sensitivity and specificity. A cut-off value of 10 mm yields high specificity but low sensitivity, whereas the reverse is true of a cut-off value of 3 mm (46). The value of MR imaging in predicting nodal involvement in rectal cancer is improved by using the border contour (sharply demarcated or irregular border) and signal intensity characteristics (homogeneity or inhomogeneity) of lymph nodes instead of size criteria (85% sensitivity, 97% specificity), but morphologic criteria cannot be applied in small (<3-mm) nodes (46). Some studies have shown that lymph node–specific contrast agents may aid in the detection of small tumor deposits, and that mesorectal lymph nodes can be characterized with use of ultrasmall superparamagnetic iron oxide particles (47–49). These particles, which are phagocytosed by nodal macrophages, produce susceptibility effects and result in signal intensity loss in normal nodes on T2- or T2*-weighted MR images. In nodes that are totally or partially replaced by tumor, the macrophage-depleted tumor-bearing areas demonstrate little susceptibility effect and retain relatively high signal intensity.

Nodal staging with ultrasmall superparamagnetic iron oxide particles has a sensitivity and specificity of approximately 95% for detecting malignant lymph nodes in patients with primary rectal cancer (47–49).

The problem for clinical application is the limited commercial availability of ultrasmall superparamagnetic iron oxide particles; the application for marketing authorization has recently been withdrawn in Europe, and approval is still pending in the United States (50).

Thin-section MR imaging performed before and after CRT provides an opportunity to observe changes in the number, size, distribution, and morphologic features of mesorectal lymph nodes. Accurate assessment of the regression of poor-prognosis stage N2 disease to stage N0 or N1 can indicate effective therapy. A change in the morphologic appearance of mesorectal lymph nodes could also result, a finding that is in keeping with mucinous change (see Fig E5 [online]) (40). Neoadjuvant CRT results in a decrease in the size and number of mesorectal lymph nodes and, after long-course CRT nodal downstaging, reportedly occurs in up to 60% of patients (26,51).

To select patients for local excision after CRT, both a residual tumor (ypT0–T2) limited to the bowel wall and a negative lymph-node status (ypN0) are essential. With a low prevalence of malignant nodes after CRT in contrast to the

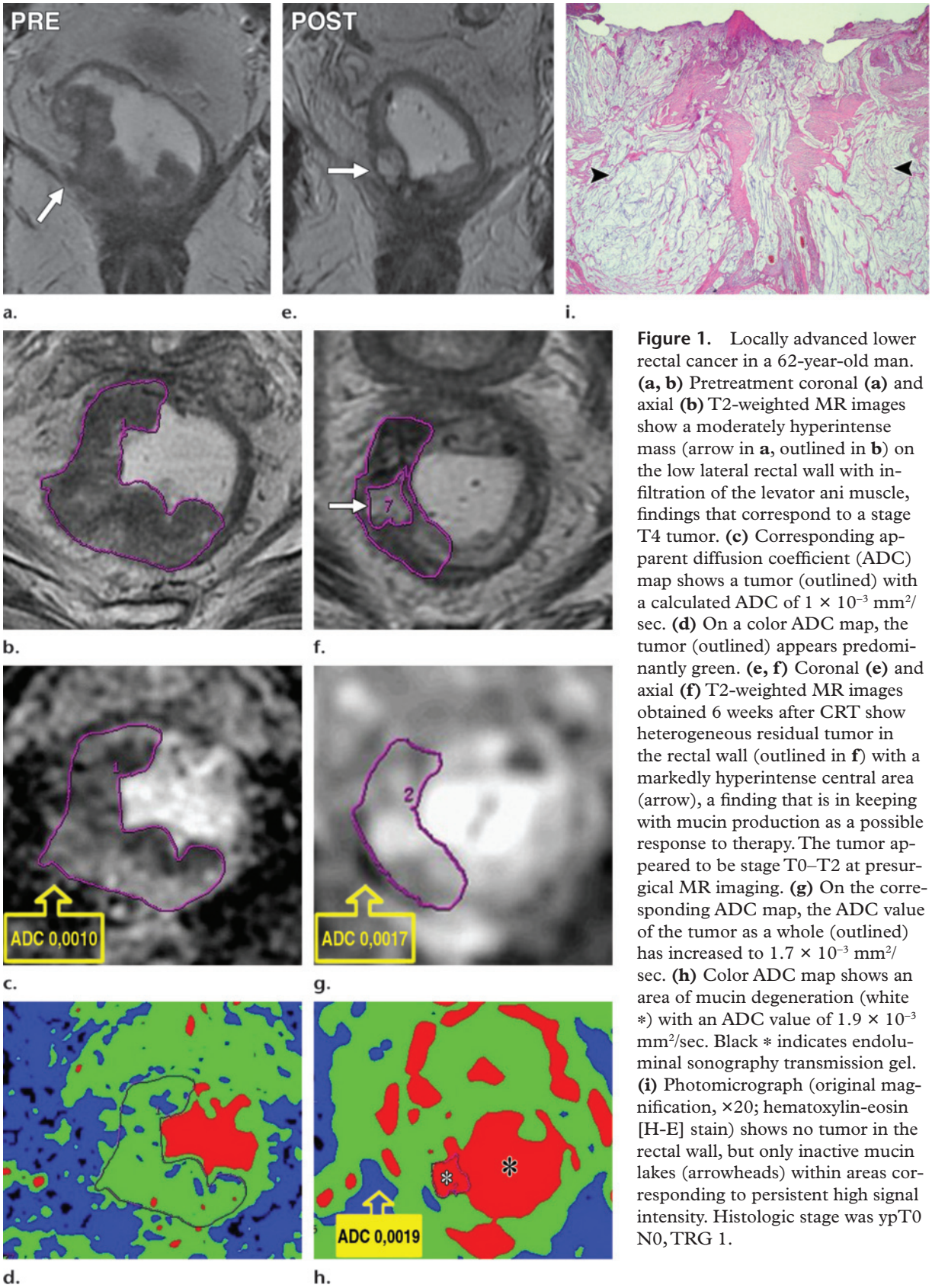

Figure 1. Locally advanced lower rectal cancer in a 62-year-old man. **(a, b)** Pretreatment coronal **(a)** and axial **(b)** T2-weighted MR images show a moderately hyperintense mass (arrow in **a**, outlined in **b**) on the low lateral rectal wall with infiltration of the levator ani muscle, findings that correspond to a stage T4 tumor. **(c)** Corresponding apparent diffusion coefficient (ADC) map shows a tumor (outlined) with a calculated ADC of 1×10^{-3} mm^2/sec. **(d)** On a color ADC map, the tumor (outlined) appears predominantly green. **(e, f)** Coronal **(e)** and axial **(f)** T2-weighted MR images obtained 6 weeks after CRT show heterogeneous residual tumor in the rectal wall (outlined in **f**) with a markedly hyperintense central area (arrow), a finding that is in keeping with mucin production as a possible response to therapy. The tumor appeared to be stage T0–T2 at presurgical MR imaging. **(g)** On the corresponding ADC map, the ADC value of the tumor as a whole (outlined) has increased to 1.7×10^{-3} mm^2/sec. **(h)** Color ADC map shows an area of mucin degeneration (white *) with an ADC value of 1.9×10^{-3} mm^2/sec. Black * indicates endoluminal sonography transmission gel. **(i)** Photomicrograph (original magnification, ×20; hematoxylin-eosin [H-E] stain) shows no tumor in the rectal wall, but only inactive mucin lakes (arrowheads) within areas corresponding to persistent high signal intensity. Histologic stage was ypT0 N0, TRG 1.

Figure 2. Stage T1 N1 rectal cancer in a 54-year-old man prior to surgery. **(a)** Axial T2-weighted MR image shows a huge tumor (outlined) on the left lateral rectal wall, protruding into the rectal lumen and invading the rectal wall without infiltrating the perirectal fat. It is difficult to determine whether the muscular layer (arrow), which appears thinned, is infiltrated or spared. **(b)** On a diffusion-weighted image obtained at a *b* value of 1000 sec/mm^2, the tumor (outlined) appears hyperintense. **(c)** Corresponding ADC map shows the tumor (outlined) as a hypointense area with an ADC value of 1.2×10^{-3} mm^2/sec. **(d)** On a sagittal inverted maximum intensity projection diffusion-weighted MR image obtained at a high *b* value, the tumor (white arrow) appears dark, with a second dark area seen cranially (black arrow). **(e)** Sagittal MR image shows an enlarged inhomogeneous lymph node (arrow), a finding that corresponds to the dark area seen cranially in **d**. The ADC value of the lymph node is 1.2×10^{-3} mm^2/sec. **(f, g)** Photomicrographs (original magnification, ×20; H-E stain) show T1 adenocarcinoma with high cellularity (∗ in **f**) and a metastatic node **(g)**.

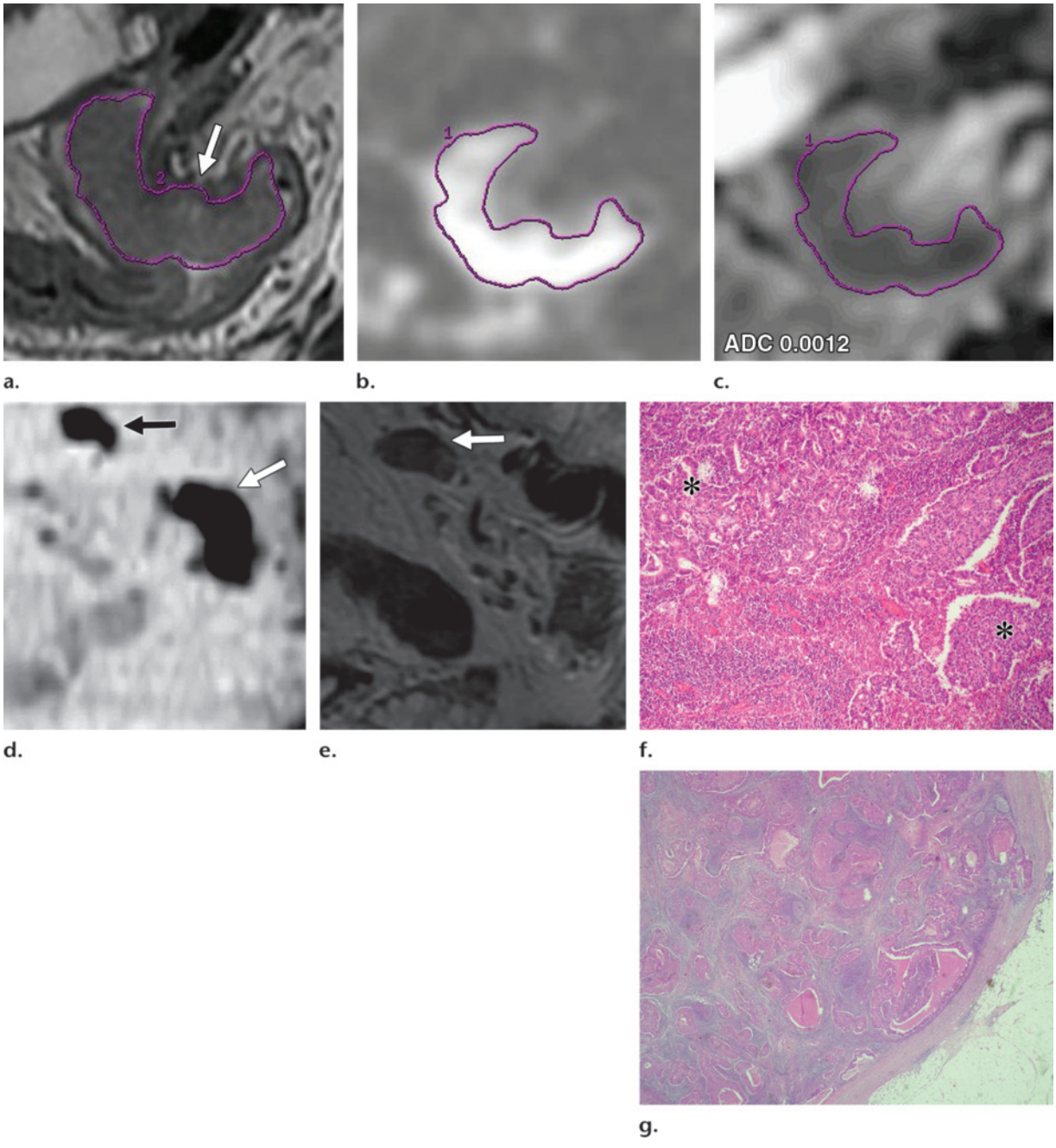

time of primary staging, the morphologic and size (short axis >5 mm) MR imaging criteria have a sensitivity and specificity of about 80%, resulting in frequent overstaging (26,40,50).

Diffusion-weighted MR Imaging Features

Diffusion-weighted imaging derives its image contrast from differences in the motion of water molecules in various tissues. The degree of restriction to water diffusion in biologic tissue is inversely correlated with cellular density and the integrity of cell membranes. The motion of water molecules is more restricted in tissues with high cellular density and intact cell membranes (eg, tumor tissue); in areas of low cellular density, or where the cell membrane has been breached, the motion of water molecules is less restricted (52). The diffusion sensitivity is easily varied by changing the parameter known as the *b* value. Water molecules with a high degree of motion or a great diffusion distance (eg, within the intravascular space) will have decreased signal at low *b* values (eg, *b* = 50–100 sec/mm^2); thus, diffusion-weighted data acquired over a range of low *b* values have decreased signal due to perfusion. In contrast, high *b* values (eg, *b* = 1000 sec/mm^2) are usually required to perceive slow-moving water molecules or small diffusion distances, both of which show more gradual decreases in signal with increasing *b* values. Axial diffusion-weighted images were obtained with a 1.5-T unit (Horizon Advantage, GE Medical Systems) using single-shot echoplanar sequences with the following parameters: >8000/minimum, eight signals averaged, 40-cm FOV, 128 × 128 matrix, 4-mm section thickness, and 0.5-mm intersection gap. With diffusion-weighted imaging performed at different *b* values (0, 600, and 1000 sec/mm^2), quantitative analysis is possible. The ADC is calculated for each pixel of the image and displayed on a parametric map. For image analysis, the data are transferred to a GE Advantage workstation and analyzed using the FuncTool dynamic analysis tool. Regions of interest (ROIs) are drawn manually on the ADC map based on the corresponding axial T2-weighted images, and the oblique high-resolution T2-weighted images are used to identify the tumor. The ADC value for a tumor is calculated as the median value of four to six measurements. We use more *b* values to reduce the error in ADC calculation, thereby allowing more meaningful comparison of results.

High-*b*-value diffusion-weighted MR imaging has shown sufficient diagnostic capacity for helping detect colorectal cancer, as reflected in its high sensitivity (91%) and specificity (100%) (53).

Diffusion-weighted MR imaging might provide images with improved signal-to-noise ratios; reversal of the contrast in these images results in black-and-white images whose contrast characteristics closely resemble those of PET scans (Fig 2) (54).

Diffusion-weighted MR imaging would be effective for the pretreatment prediction of treatment outcome, since the mean pretreatment tumor ADC correlates with the degree of tumor response after CRT and patients who respond to treatment seem to have a lower ADC at presentation than do those who do not respond (55). Therefore, the association between high tumor ADC and poor response is consistent with the known relationship between necrosis and poor response to cancer treatment (see Fig E6 [online]).

The capacity of high-*b*-value diffusion-weighted MR imaging to provide more information about the slow-moving water molecules enhances the sensitivity of this technique for the detection, in the early stages of treatment, of relatively small effects such as modified permeability of cell membranes, cell swelling, and early cell lysis and apoptosis-induced cell death.

Diffusion-weighted images obtained for monitoring radiation-induced changes in a colorectal tumor model, HT29 xenografts in mice, showed that increased tumor ADC was related to changes in the water content of tumors and tumor viability. Viable tumor cells with intact membranes restrict water diffusion, whereas necrotic tumors have disrupted membranes, resulting in increased water diffusion (56).

Disrupted membranes increase the extracellular volume due to elevated membrane permeability; thus, the increase in tumor ADC at day 11 (+11.14%) is probably the result of irreparable radiation-induced DNA damage (Fig 3) (56). As a tumor responds to treatment, the ADC is likely to rise at first, but reequilibrium may occur after a time, leading to a decrease in ADC at the end of treatment (Fig 3) (52). CRT leads to increased interstitial fibrosis with resorption of extracellular fluid at the end of treatment as documented at postsurgical examination (Figs 4–6). In an experimental study, Hein et al (57) compared changes

Teaching Point

Figure 3. Stage T3 lower rectal cancer that responded to treatment in a 45-year-old woman. **(a–c)** On axial T2-weighted MR images obtained before **(a)**, during **(b)**, and after **(c)** treatment, the tumor (outlined, arrows) demonstrates progressive shrinkage and signal intensity reduction. **(d–f)** On the corresponding ADC maps, the mean ADC value of the tumor (outlined) increases from 1.1×10^{-3} mm²/sec prior to treatment **(d)** to 1.5×10^{-3} mm²/sec in the second week of treatment **(e)**, then decreases to 1.4×10^{-3} mm²/sec at the end of treatment **(f)**. The histologic stage was ypT2 N0, TRG 2. **(g, h)** On axial inverted diffusion-weighted images obtained before **(g)** and during **(h)** treatment, the tumor (arrow) appears dark prior to treatment, indicating a low ADC value, with an increase in the ADC value during treatment. **(i, j)** FDG PET–computed tomographic (CT) images obtained before **(i)** and during **(j)** treatment show qualitative and semiquantitative metabolic response in the second week (60% decrease in maximum standardized uptake value [SUV_{max}] compared with the pretreatment SUV_{max}). Note the concordance between the inverted diffusion-weighted **(h)** and FDG PET/CT **(j)** images obtained during treatment.

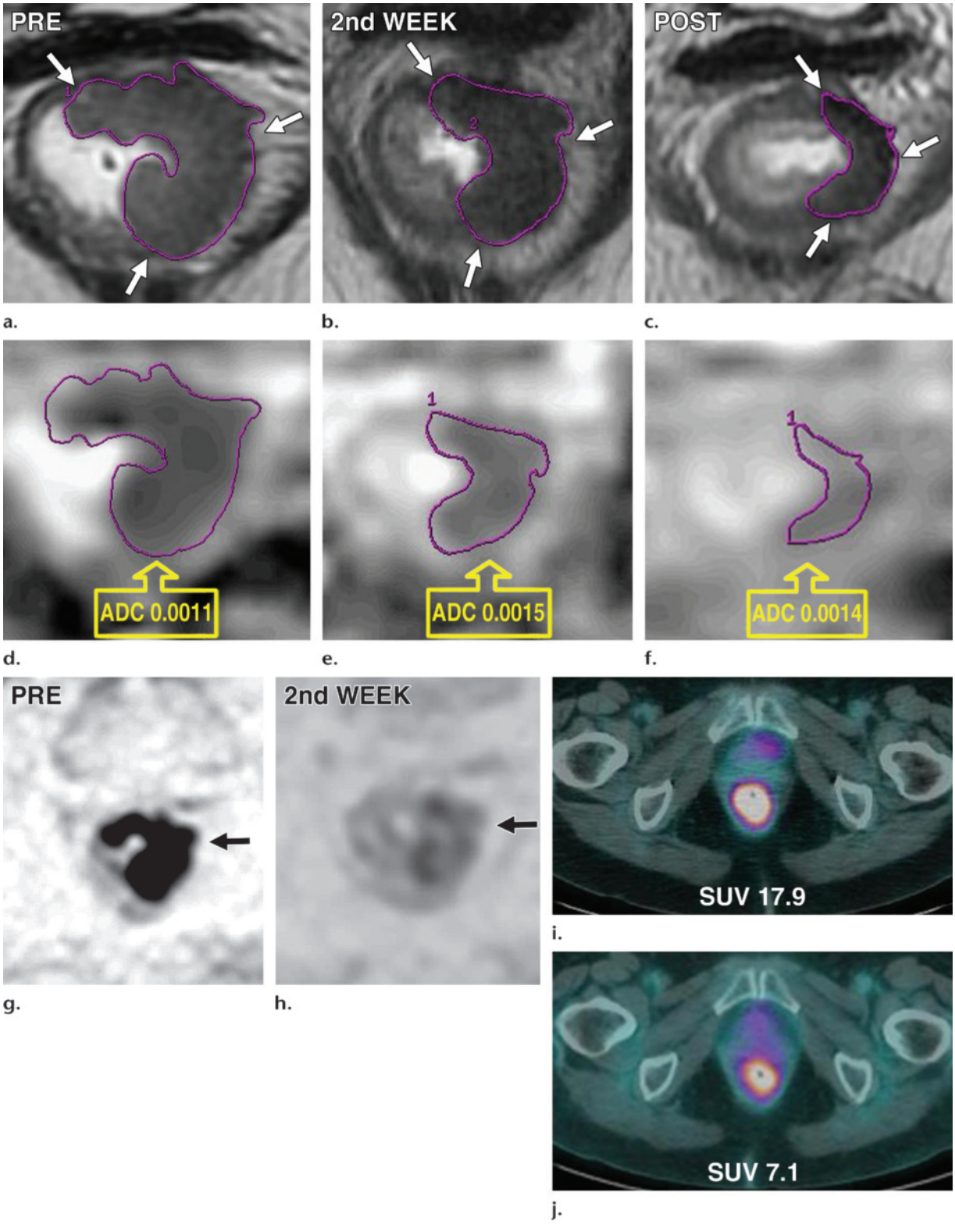

Figures 4, 5. Locally advanced midrectal cancer in a 54-year-old woman. **(4)** Oblique high-resolution T2-weighted MR images obtained before **(a)** and during **(b)** treatment show a tumor (outlined) that extends into the surrounding mesorectal fat through the perirectal fascia (black arrows), a finding that may represent CRM involvement. Note the round, ill-defined, isointense lymph node in the mesorectum abutting the mesorectal fascia (white arrow). The lymph node decreases in size during treatment. **(c)** Oblique high-resolution T2-weighted MR image obtained after treatment shows a 90% reduction in tumor volume (cf **a**). However, a focal, inhomogeneous residual tumor that reaches the perirectal fascia persists in the posterior and left mesorectum (arrows). The lymph node seen before and during treatment has disappeared. **(5)** Axial diffusion-weighted images (b = 1000 sec/mm^2) obtained before **(a)** and during **(b)** treatment show the tumor and lymph node (outlined manually using the corresponding T2-weighted images) with high signal intensity. **(c, d)** On the corresponding ADC maps, the tumor and lymph node (outlined) have low signal intensity. Their median ADC value increases from 0.7 × 10^{-3} mm^2/sec before treatment **(c)** to 1.1 × 10^{-3} mm^2/sec during treatment **(d)**, indicating a possible early response. **(e)** Axial diffusion-weighted image (b = 1000 sec/mm^2) obtained after treatment shows the tumor (outlined) with a focal hyperintense area close to the mesorectal fascia (arrow). The lymph node seen earlier is not visible. **(f)** On the corresponding ADC map, the tumor as a whole (outlined) has an ADC value of 1.2 × 10^{-3} mm^2/sec. The focal hyperintense area seen in **e** persists posteriorly as an area of restricted diffusion (arrow) and has an ADC value of 0.9 × 10^{-3} mm^2/sec.

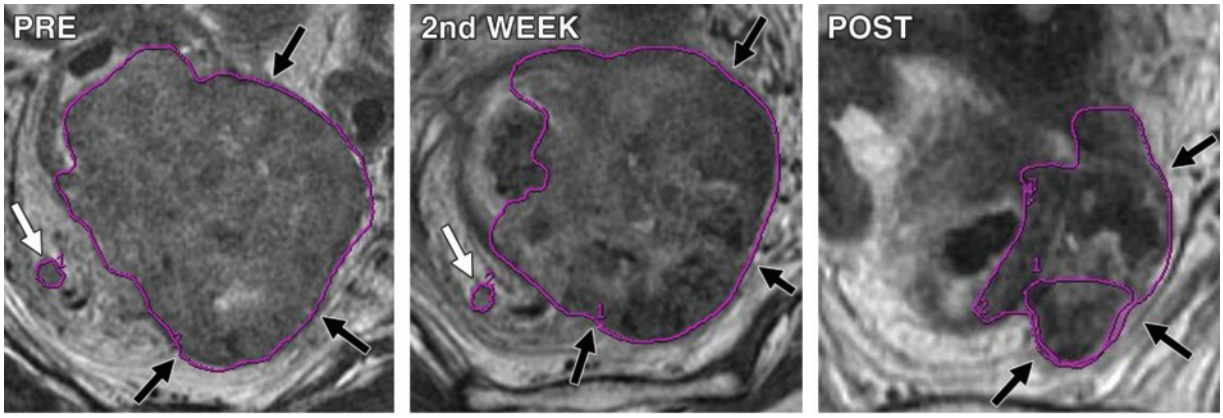

4a. 4b. 4c.

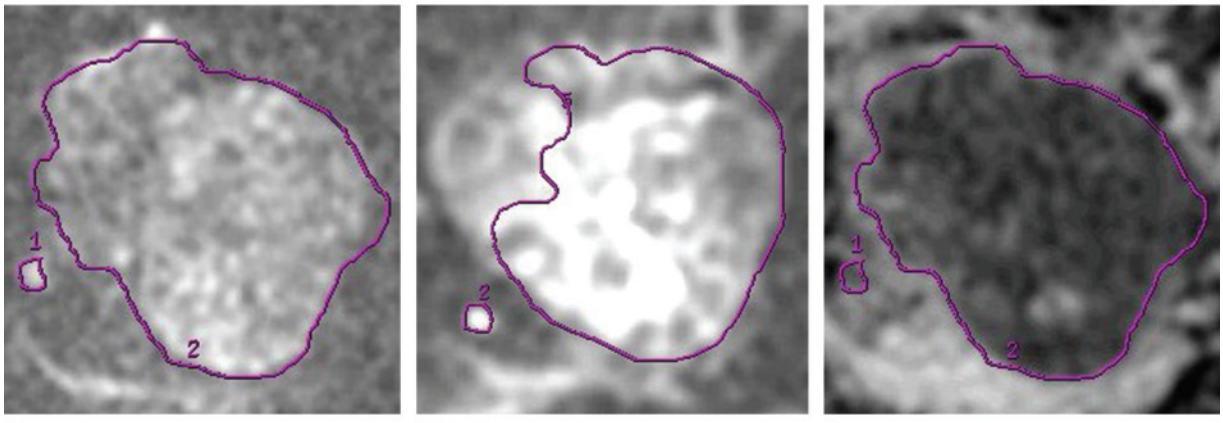

5a. 5b. 5c.

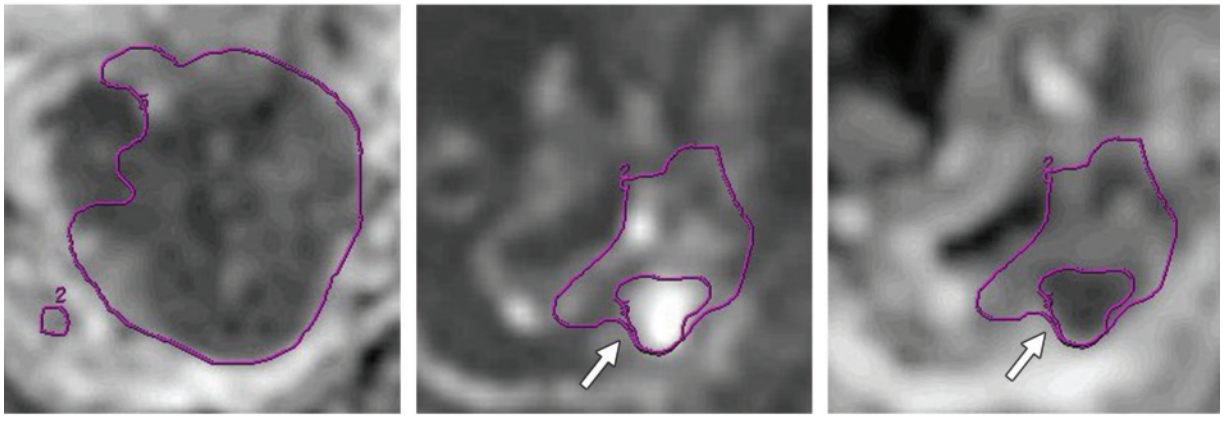

5d. 5e. 5f.

Figure 6. Diffusion-weighted MR imaging versus FDG PET/CT in the same patient as in Figures 4 and 5. **(a, b)** Axial inverted diffusion-weighted MR images obtained before **(a)** and during **(b)** treatment show a tumor that appears as an area that is moderately dark and inhomogeneous, respectively. **(c, d)** Corresponding FDG PET/CT images show an increase in the SUV_{max} value. **(e)** Axial inverted diffusion-weighted MR image obtained at the end of treatment shows a dark area of restricted diffusion posteriorly (white arrow) and an area of high diffusion anteriorly (black arrow). **(f)** On the corresponding FDG PET/CT image, there is no uptake in the area of restricted diffusion (white arrow). However, there is focal uptake in the area with a high ADC value (black arrow). **(g)** Photomicrograph (original magnification, ×20; H-E stain) shows prevalent fibrosis in the posterior mesorectum (white arrow) and prevalent inflammatory tissue anteriorly (black arrow). No CRM involvement is seen. Histologic analysis revealed a small cluster of residual cancer cells in the mesorectum (pT3 N0, TRG 3). The association between findings at diffusion-weighted imaging and FDG PET/CT in this case was useful for predicting a clear CRM, thereby avoiding the misinterpretation of high residual FDG uptake anteriorly and the area of restricted diffusion posteriorly as residual tumor abutting the mesorectal fascia.

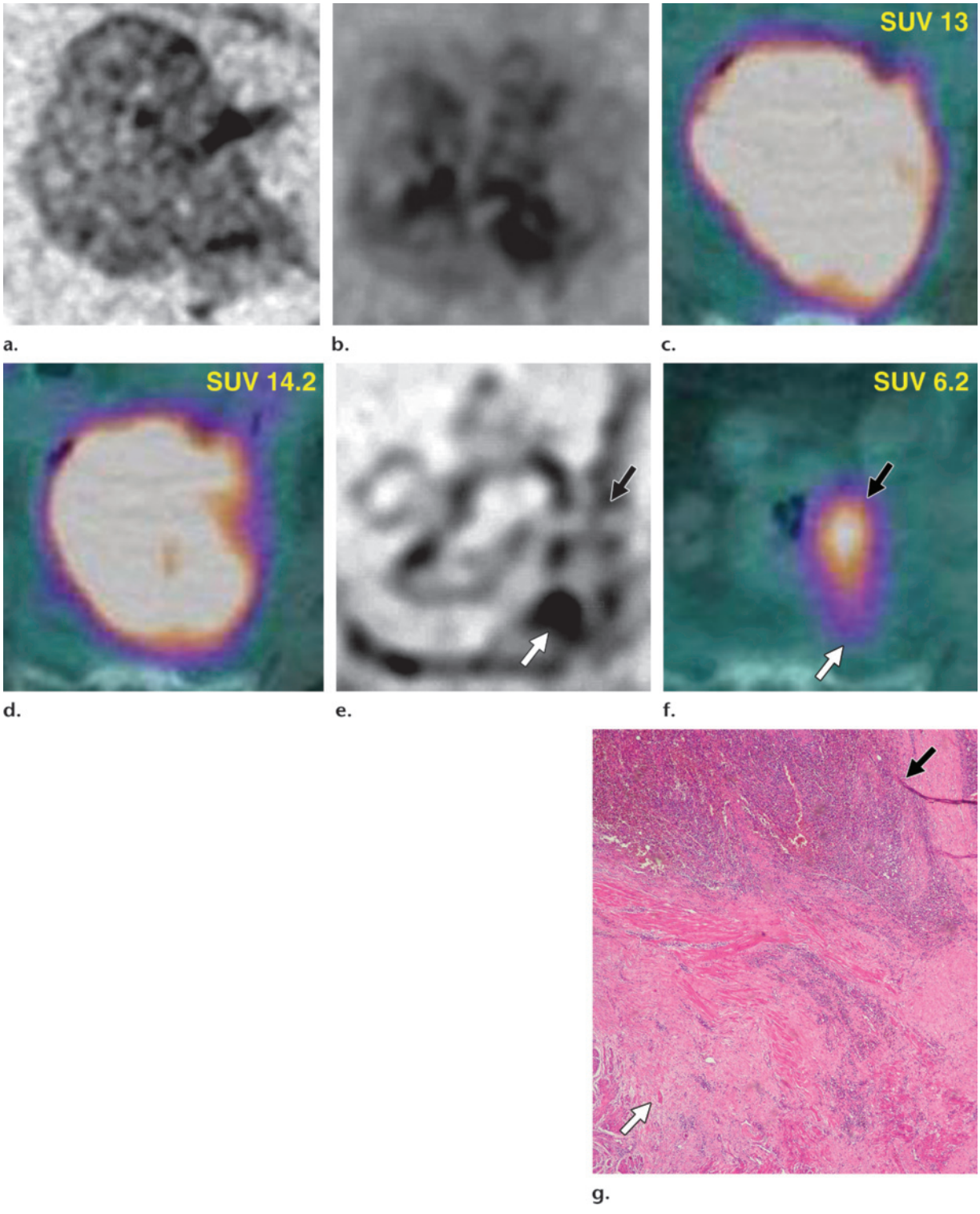

at diffusion-weighted imaging detected in vivo with histologic changes observed in excised tissue specimens and reported that the postirradiation ingrowth of fibrosis restricting water mobility was accompanied by decreased tumor ADC. Many tumors develop peritreatment areas of inflammation, thereby increasing local metabolism, which is problematic for PET studies. In our experience, tumor response as fibroinflammatory tissues could increase ADC value at the end of treatment as mucinous differentiation (Fig 1). A comparison of morphologic and functional MR images could help minimize underestimation of response due to morphologic misinterpretation of hyperintensity as residual cancer, which has low ADC values (Figs 4–6).

The combination of diffusion-weighted MR imaging and morphologic imaging criteria is useful in distinguishing malignant from benign small (subcentimetric) lymph nodes in head and squamous cell carcinoma. Lower ADC values correspond with a higher probability of lymph node metastases (cut-off value, 1.0×10^{-3} mm/sec) (58,59).

Recently, diffusion-weighted MR imaging demonstrated a sensitivity of 80%, a specificity of 76.9%, and an accuracy of 78.3% in detecting regional metastatic lymph nodes in untreated rectal cancer (short axis ≥1 cm or a cluster of three nodes, irrespective of their size) (60). We evaluate the lymph nodes with a short-axis diameter of 4 mm or more with diffusion-weighted imaging and compare these findings with morphologic findings obtained at high-resolution T2-weighted imaging (Figs 4, 5; see also Fig E7 [online]). The corresponding T2-weighted images are observed in transverse orientation to assist in identifying the lymph nodes. Although diffusion-weighted imaging takes less than 5 minutes, it must be said that evaluating all lymph nodes at the MR imaging workstation is time consuming.

Metabolic Activity at FDG PET/CT

Functional imaging with PET/CT provides diagnostic and prognostic information based on the metabolic activity of malignant tissue. Currently, there is a growing interest in prognostic stratification and response treatment prediction with PET/CT early in the course of therapy.

In vivo FDG PET/CT of tumor cells is based on the cells' increased glycolysis rate, and the rate of increase correlates with growth rate.

FDG uptake in tissues (SUV is a semiquantitative measurement calculated as the tissue radioactivity concentration divided by the injected activity and multiplied by body weight) can be accurately quantified, and sequential determination of this parameter has been shown to help predict response to chemotherapy or radiation therapy, thereby supporting the hypothesis that metabolic changes assessed with FDG PET/CT are not associated with, but may precede, therapy-induced changes in tumor size.

In the staging of primary rectal cancer, FDG PET/CT may influence management in 15.7% of patients, mainly due to the identification of unknown metastatic disease and the extension of the neoadjuvant radiation therapy field (61).

However, FDG PET/CT is not routinely recommended for rectal cancer staging (62)—except in advanced rectal cancer, for unequivocal characterization of lesions before resection of metastatic disease or identification of new lesions in cases of planned metastasis resection.

Baseline FDG PET/CT is necessary for monitoring metabolic response to neoadjuvant therapy: The decrease in glucose utilization during therapy correlates with a reduction in the number of viable tumor cells, as is evident from comparison with pathologic specimens. In 1999, the European Organization for Research and Treatment of Cancer published recommendations for metabolic response assessment (63). As a criterion for partial metabolic response, it proposed a minimum reduction of 15%–25% in SUV_{max} after one treatment cycle and a greater than 25% reduction after two or more treatment cycles (63). However, the threshold for significant SUV reduction during and after treatment still needs to be revised, and several factors such as type of tumor, type of treatment, and timing of evaluation may influence its calculation.

Teaching Point

Several studies have compared metabolic and histopathologic tumor responses in primary rectal cancer at the end of neoadjuvant treatment, all of which found that SUV reduction is significantly greater in patients who respond to treatment (TRG 1–2) than in those who do not (TRG 3–5) (64–66).

Recently, a 66.2% decrease in SUV_{max} (percentage of SUV decrease from baseline to presurgical value) has been reported as the optimal cut-off value for differentiating patients who respond to treatment from those who do not (positive predictive value = 77%, negative predictive value = 89%) (see Figs E6 and E8 [online]) (65). A

52% decrease in SUV_{mean} and a 43% decrease in SUV_{max} on day 15 have been reported to accurately help differentiate between these two patient groups (Fig 3) (66,67). The early identification of "nonresponding" patients during the course of CRT may have clinically relevant consequences, intensifying presurgical neoadjuvant treatment in the subgroup without FDG PET/CT response.

The strength of FDG PET/CT is that it permits whole-body imaging, allowing metabolic characterization and monitoring of multiple tumor sites at the same time.

The main limitation of PET lies in the spatial resolution requirement for surgical anatomic road maps generated to plan the extent of surgical resection. The main reasons for its failure may lie in the complex tumor shapes and constitution of microscopic tumor disease scattered in the background of regressive tumor changes—quite a different scenario compared with untreated tumor. Microscopic residual tumor disease at the border of the tumor may result in underestimation of tumor volume and, therefore, overestimation of anatomic tumor response.

Confounding radiation therapy–induced effects have been reported: Residual high FDG uptake does not correlate with the percentage of viable tumor cells. Increased FDG uptake by nonneoplastic elements, such as tumor-associated macrophages and young granulation tissues, especially after radiation therapy, results in overestimation of tumor volume and, therefore, underestimation of anatomic tumor response (Fig 6) (68,69). The role of FDG PET/CT in assessing nodal involvement of the mesorectum is not clearly defined. A sensitivity of only 29% for predicting local lymph node involvement has been demonstrated (70,71) and is related to the limited spatial resolution of the currently available PET/CT scanners. In particular, partial volume averaging effect in lymph nodes with a maximum diameter of less than 1 cm and spillover effect due to high FDG uptake by the primary tumor may lead to false-negative results (see Fig E7 [online]).

Discussion

The first decade of the 21st century is witnessing a revolution in the management of rectal cancer. Although surgery is still the most important tool, the treatment has changed, and the best clinical management is increasingly being delivered by a highly skilled multidisciplinary team (9).

In this time of changing treatments, it seems clear that a common standard for large, heterogeneous patient groups must be replaced by more individualized therapies. The radiologist's role in the preoperative multidisciplinary team's decision-making process has become critical because the information provided by detailed imaging of the primary tumor guides the team in achieving better outcomes for patients with rectal cancer. In any neoadjuvant CRT, accurate restaging to assess treatment success is critical, since it can guide optimization of the surgical approach, such as sphincter-saving surgery in deep-seated tumors, less aggressive resection in initially advanced tumors, or intraoperative radiation therapy depending on tumor response. Restaging with imaging could be relevant for surgeons. The first question to be answered is, Can MR imaging help determine whether the tumor has regressed from other organs or the mesorectal fascia before standard total mesorectal excision is performed? The second question is whether MR imaging can be used prior to treatment to identify stage T3 tumors that will convert to T2 or lower-stage tumors after CRT, thereby allowing more conservative resection (26). This affects patients at both ends of the spectrum if CRT has been extraordinarily effective, so that if no visible tumor (or only minimal intramural tumor) remains, local excision can be performed, or if tumor has spread to the mesorectal fascia or beyond, radical surgery is inappropriate. Management of nonresponding tumors could change with planning of intraoperative radiation therapy. Purely anatomic MR imaging is insufficient for reliably helping assess these critical issues, and there is considerable enthusiasm for using the two functional modalities: diffusion-weighted MR imaging and FDG PET.

Functional imaging techniques that can noninvasively help monitor tumor response to treatment are highly desirable; therefore, there is great interest in integrating functional imaging into trials of chemotherapy and radiation therapy. Functional imaging has conventionally been the domain of nuclear medicine. However, radionuclide techniques have limitations, such as low spatial resolution and high cost. PET parameters are related to changes in tumor metabolism, which are not necessarily accompanied by tumor shrinkage; thus, PET is not helpful in predicting anatomic tumor changes due to its lack of spatial resolution. However, PET/CT may be useful in predicting pathologic tumor response on the basis of a significant correlation between the per-

Teaching Point

centage SUV reduction and the pathologic tumor response expressed as a TRG score (66).

Diffusion-weighted MR imaging may be an appropriate tool for monitoring the effects of treatment in vivo. Advantages of this technique are that it is completely noninvasive; does not require exposure to ionizing radiation, the injection of contrast material, or expensive investments; and does not cause patient discomfort. Another advantage of diffusion-weighted MR imaging is that it can easily be added to an MR imaging protocol because it requires only minimal additional examination time. Studies in cerebral gliomas, breast carcinoma, and advanced cervical cancers have shown that an early increase in ADC after the initiation of treatment was predictive of better treatment outcome (72–74). Changes in ADC after 2 weeks of CRT serve as an early and reproducible indication of tumor response in rectal cancer, a fact that may ultimately allow the development of individualized regimens (56,57).

The ability to distinguish residual neoplastic tissue from scarring after CRT, when presurgical restaging is being performed, is the major challenge; a clear distinction between fibrosis and residual cancer in terms of ADC changes requires further evaluation. N restaging is crucial in the restaging of rectal cancer. Nodes lying outside the mesorectal fascia may require extended lymphadenectomy to achieve tumor clearance. A node-negative status prior to surgery could result in less aggressive surgery.

To our knowledge, no data have been published concerning the accuracy of diffusion-weighted MR imaging for the post-CRT evaluation of node response in rectal cancer.

Reproducibility measurements are necessary to determine the limits of error in quantitative ADC measurements, thereby allowing a better understanding of the magnitude of change that can be confidently detected. Preliminary results have shown that a mean difference of −0.003 is considered close to zero, whereas the limits of agreement (−0.12 and 0.11) indicate the likely reproducibility of ADC measurements (95% confidence interval) (74).

Reproducibility is particularly important if diffusion-weighted imaging measurements are to be routinely used for monitoring therapeutic effects in the future. In addition, it is essential that imaging protocols and data analysis methods be standardized. Identification of the optimal criteria for prediction of response is also urgently needed. For clinical trials, it is important to understand how the ADC value of a tumor varies temporally with a given treatment.

Conclusions

Diffusion-weighted MR imaging is a useful tool for monitoring rectal cancer response after CRT. In the future, studies with large patient samples will be needed to evaluate the impact of this modality on rectal cancer restaging prior to surgery and to determine whether it can complement or even replace PET. The detection of small clusters of residual tumor cells remains a problem.

References

1. Jemal A, Murray T, Ward E, et al. Cancer statistics, 2005. CA Cancer J Clin 2005;55(1):10–30.
2. Eddy DM. Screening for colorectal cancer. Ann Intern Med 1990;113(5):373–384.
3. Sagar PM, Pemberton JH. Surgical management of locally recurrent rectal cancer. Br J Surg 1996; 83(3):293–304.
4. Brown G. Thin section MRI in multidisciplinary pre-operative decision making for patients with rectal cancer. Br J Radiol 2005;78(spec no 2): S117–S127.
5. Quirke P, Durdey P, Dixon MF, Williams NS. Local recurrence of rectal adenocarcinoma due to inadequate surgical resection: histopathological study of lateral tumour spread and surgical excision. Lancet 1986;2(8514):996–999.
6. Valentini V, Coco C, Rizzo G, et al. Outcomes of clinical T4M0 extra-peritoneal rectal cancer treated with preoperative radiochemotherapy and surgery: a prospective evaluation of a single institutional experience. Surgery 2009;145(5):486–494.
7. Kapiteijn E, Marijnen CA, Nagtegaal ID, et al. Preoperative radiation therapy combined with total mesorectal excision for resectable rectal cancer. N Engl J Med 2001;345(9):638–646.
8. Improved survival with preoperative radiation therapy in resectable rectal cancer. Swedish Rectal Cancer Trial. N Engl J Med 1997;336(14):980–987.
9. Valentini V, Beets-Tan R, Borras JM, et al. Evidence and research in rectal cancer. Radiother Oncol 2008; 87(3):449–474.
10. Brown G, Radcliffe AG, Newcombe RG, Dallimore NS, Bourne MW, Williams GT. Preoperative assessment of prognostic factors in rectal cancer using high-resolution magnetic resonance imaging. Br J Surg 2003;90(3):355–364.
11. Beets-Tan RG, Beets GL, Vliegen RF, et al. Accuracy of magnetic resonance imaging in prediction of tumour-free resection margin in rectal cancer surgery. Lancet 2001;357(9255):497–504.
12. MERCURY Study Group. Extramural depth of tumor invasion at thin-section MR in patients with rectal cancer: results of the MERCURY study. Radiology 2007;243(1):132–139.

13. Heald RJ, Ryall RD. Recurrence and survival after total mesorectal excision for rectal cancer. Lancet 1986;1(8496):1479–1482.
14. Sauer R, Becker H, Hohenberger W, et al. Preoperative versus postoperative chemoradiotherapy for rectal cancer. N Engl J Med 2004;351(17): 1731–1740.
15. Valentini V, Coco C, Minsky BD, et al. Randomized, multicenter, phase IIb study of preoperative chemoradiotherapy in T3 mid-distal rectal cancer: raltitrexed + oxaliplatin + radiotherapy versus cisplatin + 5-fluorouracil + radiotherapy. Int J Radiat Oncol Biol Phys 2008;70(2): 403–412.
16. Hiotis SP, Weber SM, Cohen AM, et al. Assessing the predictive value of clinical complete response to neoadjuvant therapy for rectal cancer: an analysis of 488 patients. J Am Coll Surg 2002; 94(2):131–135; discussion 135–136.
17. Schell SR, Zlotecki RA, Mendenhall WM, Marsh RW, Vauthey JN, Copeland EM 3rd. Transanal excision of locally advanced rectal cancers downstaged using neoadjuvant chemoradiotherapy. J Am Coll Surg 2002;194(5):584–590; discussion 590–591.
18. Coco C, Manno A, Mattana C, et al. The role of local excision in rectal cancer after complete response to neoadjuvant treatment. Surg Oncol 2007;16 (suppl 1):S101–S104.
19. Buess G. Transanal microsurgery [in German]. Langenbecks Arch Chir Suppl Kongressbd 1991: 441–447.
20. Dresen RC, Beets GL, Rutten HJ, et al. Locally advanced rectal cancer: MR imaging for restaging after neoadjuvant radiation therapy with concomitant chemotherapy. I. Are we able to predict tumor confined to the rectal wall? Radiology 2009;252(1): 71–80.
21. Habr-Gama A, Perez RO, Nadalin W, et al. Operative versus nonoperative treatment for stage 0 distal rectal cancer following chemoradiation therapy: long-term results. Ann Surg 2004; 240(4): 711–717; discussion 717–718.
22. Zhang XM, Zhang HL, Yu D, et al. 3-T MRI of rectal carcinoma: preoperative diagnosis, staging, and planning of sphincter-sparing surgery. AJR Am J Roentgenol 2008;190(5):1271–1278.
23. Brown G, Daniels IR, Richardson C, Revell P, Peppercorn D, Bourne M. Techniques and troubleshooting in high spatial resolution thin slice MRI for rectal cancer. Br J Radiol 2005;78(927): 245–251.
24. Klessen C, Rogalla P, Taupitz M. Local staging of rectal cancer: the current role of MRI. Eur Radiol 2007;17(2):379–389.
25. Kim SH, Lee JM, Lee MW, Kim GH, Han JK, Choi BI. Sonography transmission gel as endo-rectal contrast agent for tumor visualization in rectal cancer. AJR Am J Roentgenol 2008;191(1): 186–189.
26. Barbaro B, Fiorucci C, Tebala C, et al. Locally advanced rectal cancer: MR imaging in prediction of response after preoperative chemotherapy and radiation therapy. Radiology 2009;250(3): 730–739.
27. Suzuki C, Jacobsson H, Hatschek T, et al. Radiologic measurements of tumor response to treatment: practical approaches and limitations. RadioGraphics 2008;28(2):329–344.
28. World Health Organization. WHO handbook for reporting results of cancer treatment. http://whqlibdoc.who.int/publications/9241700483.pdf. Accessed March 3, 2009.
29. Therasse P, Arbuck SG, Eisenhauer EA, et al. New guidelines to evaluate the response to treatment in solid tumors. European Organization for Research and Treatment of Cancer, National Cancer Institute of the United States, National Cancer Institute of Canada. J Natl Cancer Inst 2000;92(3):205–216.
30. Shia J, Guillem JG, Moore HG, et al. Patterns of morphologic alteration in residual rectal carcinoma following preoperative chemoradiation and their association with long-term outcome. Am J Surg Pathol 2004;28(2):215–223.
31. Compton CC, Fielding LP, Burgart LJ, et al. Prognostic factors in colorectal cancer. College of American Pathologists Consensus Statement 1999. Arch Pathol Lab Med 2000;124(7):979–994.
32. Nagtegaal I, Gaspar C, Marijnen C, Van De Velde C, Fodde R, Van Krieken H. Morphological changes in tumour type after radiation therapy are accompanied by changes in gene expression profile but not in clinical behaviour. J Pathol 2004; 204(2):183–192.
33. Green JB, Timmcke AE, Mitchell WT, Hicks TC, Gathright JB Jr, Ray JE. Mucinous carcinoma: just another colon cancer? Dis Colon Rectum 1993;36 (1):49–54.
34. Umpleby HC, Ranson DL, Williamson RC. Peculiarities of mucinous colorectal carcinoma. Br J Surg 1985;72(9):715–718.
35. Mandard AM, Dalibard F, Mandard JC, et al. Pathologic assessment of tumor regression after preoperative chemoradiotherapy of esophageal carcinoma: clinicopathologic correlations. Cancer 1994;73(11): 2680–2686.
36. Vecchio FM, Valentini V, Minsky BD, et al. The relationship of pathologic tumor regression grade (TRG) and outcomes after preoperative therapy in rectal cancer. Int J Radiat Oncol Biol Phys 2005;62(3):752–760.
37. Hussain SM, Outwater EK, Siegelman ES. Mucinous versus nonmucinous rectal carcinomas: differentiation with MR imaging. Radiology 1999;213(1): 79–85.
38. Torkzad MR, Suzuki C, Tanaka S, Palmer G, Holm T, Blomqvist L. Morphological assessment of the interface between tumor and neighboring tissues, by magnetic resonance imaging, before and after radiation therapy in patients with locally advanced rectal cancer. Acta Radiol 2008;49(10): 1099–1103.
39. Vliegen RF, Beets GL, Lammering G, et al. Mesorectal fascia invasion after neoadjuvant chemotherapy and radiation therapy for locally advanced rectal cancer: accuracy of MR imaging for prediction. Radiology 2008;246(2):454–462.
40. Koh DM, Chau I, Tait D, Wotherspoon A, Cunningham D, Brown G. Evaluating mesorectal lymph

nodes in rectal cancer before and after neoadjuvant chemoradiation using thin-section T2-weighted magnetic resonance imaging. Int J Radiat Oncol Biol Phys 2008;71(2):456–461.
41. Taylor FG, Swift RI, Blomqvist L, Brown G. A systematic approach to the interpretation of preoperative staging MRI for rectal cancer. AJR Am J Roentgenol 2008;191(6):1827–1835.
42. Rullier A, Laurent C, Vendrely V, Le Bail B, Bioulac-Sage P, Rullier E. Impact of colloid response on survival after preoperative radiation therapy in locally advanced rectal carcinoma. Am J Surg Pathol 2005; 29(5):602–606.
43. Allen SD, Padhani AR, Dzik-Jurasz AS, Glynne-Jones R. Rectal carcinoma: MRI with histologic correlation before and after chemoradiation therapy. AJR Am J Roentgenol 2007;188(2):442–451.
44. Chen CC, Lee RC, Lin JK, Wang LW, Yang SH. How accurate is magnetic resonance imaging in restaging rectal cancer in patients receiving preoperative combined chemoradiotherapy? Dis Colon Rectum 2005;48(4):722–728.
45. Kuo LJ, Chern MC, Tsou MH, et al. Interpretation of magnetic resonance imaging for locally advanced rectal carcinoma after preoperative chemoradiation therapy. Dis Colon Rectum 2005;48(1): 23–28.
46. Brown G, Richards CJ, Bourne MW, et al. Morphologic predictors of lymph node status in rectal cancer with use of high-spatial-resolution MR imaging with histopathologic comparison. Radiology 2003; 227(2):371–377.
47. Koh DM, Hughes M, Husband JE. Cross-sectional imaging of nodal metastases in the abdomen and pelvis. Abdom Imaging 2006;31(6):632–643.
48. Koh DM, Brown G, Temple L, et al. Rectal cancer: mesorectal lymph nodes at MR imaging with USPIO versus histopathologic findings—initial observations. Radiology 2004;231(1):91–99.
49. Lahaye MJ, Engelen SM, Kessels AG, et al. USPIO-enhanced MR imaging for nodal staging in patients with primary rectal cancer: predictive criteria. Radiology 2008;246(3):804–811.
50. Lahaye MJ, Beets GL, Engelen SME, et al. Locally advanced rectal cancer: MR imaging for restaging after neoadjuvant radiation therapy with concomitant chemotherapy. II. What are the criteria to predict involved lymph nodes? Radiology 2009;252(1): 81–91.
51. Valentini V, Coco C, Cellini N, et al. Preoperative chemoradiation with cisplatin and 5-fluorouracil for extraperitoneal T3 rectal cancer: acute toxicity, tumor response, sphincter preservation. Int J Radiat Oncol Biol Phys 1999;45(5):1175–1184.
52. Koh DM, Collins DJ. Diffusion-weighted MRI in the body: applications and challenges in oncology. AJR Am J Roentgenol 2007;188(6):1622– 1635.
53. Ichikawa T, Erturk SM, Motosugi U, et al. High-B-value diffusion-weighted MRI in colorectal cancer. AJR Am J Roentgenol 2006;187(1):181–184.
54. Takahara T, Imai Y, Yamashita T, Yasuda S, Nasu S, Van Cauteren M. Diffusion weighted whole body imaging with background body signal suppression (DWIBS): technical improvement using free breathing, STIR and high resolution 3D display. Radiat Med 2004;22(4):275–282.
55. Dzik-Jurasz A, Domenig C, George M, et al. Diffusion MRI for prediction of response of rectal cancer to chemoradiation. Lancet 2002;360 (9329):307–308.
56. Seierstad T, Røe K, Olsen DR. Noninvasive monitoring of radiation-induced treatment response using proton magnetic resonance spectroscopy and diffusion-weighted magnetic resonance imaging in a colorectal tumor model. Radiother Oncol 2007; 85 (2):187–194.
57. Hein PA, Kremser C, Judmaier W, et al. Diffusion-weighted magnetic resonance imaging for monitoring diffusion changes in rectal carcinoma during combined, preoperative chemoradiation: preliminary results of a prospective study. Eur J Radiol 2003;45(3):214–222.
58. Vandecaveye V, De Keyzer F, Nuyts S, et al. Detection of head and neck squamous cell carcinoma with diffusion weighted MRI after (chemo)radiation therapy: correlation between radiologic and histopathologic findings. Int J Radiat Oncol Biol Phys 2007;67(4):960–971.
59. de Bondt RB, Hoeberigs MC, Nelemans PJ, et al. Diagnostic accuracy and additional value of diffusion-weighted imaging for discrimination of malignant cervical lymph nodes in head and neck squamous cell carcinoma. Neuroradiology 2009;51 (3):183–192.
60. Ono K, Ochiai R, Yoshida T, et al. Comparison of diffusion-weighted MRI and 2-[fluorine-18]-fluoro-2-deoxy-D-glucose positron emission tomography (FDG-PET) for detecting primary colorectal cancer and regional lymph node metastases. J Magn Reson Imaging 2009;29(2):336–340.
61. Vriens D, de Geus-Oei LF, van der Graaf WTA, Oyen WJI. Tailoring therapy in colorectal cancer by PET-CT. Q J Nucl Med Mol Imaging 2009;53(2): 224–244.
62. Glimelius B, Oliveira J; ESMO Guidelines Working Group. Rectal cancer: ESMO clinical recommendations for diagnosis, treatment and follow-up. Ann Oncol 2009;20(suppl 4):54–56.
63. Young H, Baum R, Cremerius U, et al. Measurement of clinical and subclinical tumour response using [18F]-fluorodeoxyglucose and positron emission tomography: review and 1999 EORTC recommendations. European Organization for Research and Treatment of Cancer (EORTC) PET Study Group. Eur J Cancer 1999;35:1773–1782.
64. Calvo FA, Domper M, Matute R, et al. 18F-FDG positron emission tomography staging and restaging in rectal cancer treated with preoperative chemoradiation. Int J Radiat Oncol Biol Phys 2004;58(2): 528–535.
65. Capirci C, Rampin L, Erba PA, et al. Sequential FDG-PET/CT reliably predicts response of locally advanced rectal cancer to neo-adjuvant chemo-radiation therapy. Eur J Nucl Med Mol Imaging 2007; 34(10):1583–1593.

66. Janssen MH, Ollers MC, Riedl RG, et al. Accurate prediction of pathological rectal tumor response after two weeks of preoperative radiochemotherapy using 18F-fluorodeoxyglucose-positron emission tomography-computed tomography imaging. Int J Radiat Oncol Biol Phys. 2009 Jul 29. [Epub ahead of print]
67. Cascini GL, Avallone A, Delrio P, et al. 18F-FDG PET is an early predictor of pathologic tumor response to preoperative radiochemotherapy in locally advanced rectal cancer. J Nucl Med 2006;47(8):1241–1248.
68. Kubota R, Yamada S, Kubota K, Ishiwata K, Tamahashi N, Ido T. Intratumoral distribution of fluorine-18-fluorodeoxyglucose in vivo: high accumulation in macrophages and granulation tissues studied by microautoradiography. J Nucl Med 1992;33(11):1972–1980.
69. Capirci C, Rubello D, Chierichetti F, et al. Restaging after neoadjuvant chemoradiotherapy for rectal adenocarcinoma: role of F18-FDG PET. Biomed Pharmacother 2004;58(8):451–457.
70. Heriot AG, Hicks RJ, Drummond EG, et al. Does positron emission tomography change management in primary rectal cancer? a prospective assessment. Dis Colon Rectum 2004;47(4):451–458.
71. Abdel-Nabi H, Doerr RJ, Lamonica DM, et al. Staging of primary colorectal carcinomas with fluorine-18 fluorodeoxyglucose whole-body PET: correlation with histopathologic and CT findings. Radiology 1998;206(3):755–760.
72. Mardor Y, Pfeffer R, Spiegelmann R, et al. Early detection of response to radiation therapy in patients with brain malignancies using conventional and high b-value diffusion-weighted magnetic resonance imaging. J Clin Oncol 2003;21(6):1094–1100.
73. Theilmann RJ, Borders R, Trouard TP, et al. Changes in water mobility measured by diffusion MRI predict response of metastatic breast cancer to chemotherapy. Neoplasia 2004;6(6):831–837.
74. Harry VN, Semple SI, Gilbert FJ, Parkin DE. Diffusion-weighted magnetic resonance imaging in the early detection of response to chemoradiation in cervical cancer. Gynecol Oncol 2008;111(2):213–220.

Restaging Locally Advanced Rectal Cancer with MR Imaging after Chemoradiation Therapy

Brunella Barbaro, MD • Renata Vitale, MD • Lucia Leccisotti, MD • Fabio M. Vecchio, MD • Luisa Santoro, MD • Vincenzo Valentini, MD • Claudio Coco, MD • Fabio Pacelli, MD • Antonio Crucitti, MD • Roberto Persiani, MD • Lorenzo Bonomo, MD

RadioGraphics 2010; 30:699–721 • **Published online** 10.1148/rg.303095085 • **Content Codes:** GI MR OI RO

Page 701
Some researchers are now addressing organ preservation by using preoperative CRT followed by local excision in patients in whom *(a)* CRT has led to downstaging of tumors to lesions confined to the rectal wall, and *(b)* there are no longer any involved lymph nodes (17,18).

Page 704
A reasonable level of accuracy has been achieved with phased-array MR imaging when the end point is differentiating ypT0–T2 tumors from ypT3 tumors, especially when morphologic and volumetric criteria are combined (20,26).

Page 707
As a tumor responds to treatment, the ADC is likely to rise at first, but reequilibrium may occur after a time, leading to a decrease in ADC at the end of treatment (Fig 3) (52).

Page 711
Several studies have compared metabolic and histopathologic tumor responses in primary rectal cancer at the end of neoadjuvant treatment, all of which found that SUV reduction is significantly greater in patients who respond to treatment (TRG 1–2) than in those who do not (TRG 3–5) (64–66).

Page 712
PET parameters are related to changes in tumor metabolism, which are not necessarily accompanied by tumor shrinkage; thus, PET is not helpful in predicting anatomic tumor changes due to its lack of spatial resolution.